Proceedings of the Institute of Acoustics

FEEDBACK CONTROL LAWS FOR INERTIAL ACTUATORS

C.González Díaz ISVR, University of Southampton, Southampton, UK
P.Gardonio ISVR, University of Southampton, Southampton, UK

1 INTRODUCTION

In many engineering systems it is important to control the transmission of vibration from a source of disturbance to other devices or to the environment in order to prevent discomfort and loss of efficiency. In particular, vibration of panels and shell structures may generate high levels of noise which could be a problem in many applications, mainly in transportation vehicles such as aircrafts, helicopters, cars, trains, etc. The background of this study is the control of vibration of thin panels to avoid excessive vibration and sound radiation levels. Vibration and sound radiation control can be achieved with passive means such as mass damping and stiffness treatments applied on the radiating structure[1]. These methods have been proved to be efficient in the high audio frequency range. However, they tend to be less effective in the low audio frequency range, where the mechanical responses of structures are characterised by well–separated resonances. In order to control low frequency vibration and sound radiation, active control methods have been considered[2]. Frequently both passive and active systems are used together to reduce transmitted vibration and radiated sound.

Active control systems can be divided into two groups: feedforward and feedback control systems. Feedforward control systems require a reference signal well correlated to the disturbance to be controlled. Thus they normally provide good control effects for tonal disturbances that can be easily characterised far in advance[3,4]. For random disturbances, feedback control schemes should be utilized. These systems can provide good control performance regardless the type of disturbance to be controlled provided the sensor and actuator transducers are collocated and dual so that large feedback control gains can be implemented with no stability problems[5,6]. Feedback control systems for vibro-acoustic control can be classified in three categories: a) Multiple Input Multiple Output (MIMO) systems with fully coupled arrays of error sensor and actuators, b) Decentralised MIMO feedback control schemes with arrays of independent sensor–actuator pairs, and c) Single Input Single Output (SISO) active feedback control schemes, using distributed sensor–actuator pairs.

Fully coupled MIMO feedback systems are difficult to implement in practice, since a reliable model of the response functions between all sensors and actuators is required by the controller[5,6]. MIMO decentralised control systems have been shown to give good control performance which are comparable to those that would be obtained from an ideal fully coupled MIMO feedback control system[7,8]. The implementation of decentralised MIMO system is much simpler than that of fully coupled systems, since simple SISO feedback loops need to be implemented. Elliott at al.[9] have shown that, provided the sensor–actuator pairs are dual and collocated[10,11], the decentralised MIMO system is bound to be stable if direct velocity control is implemented[12]. Therefore, the main issue of decentralised MIMO control is concerned with the design of collocated and dual sensor–actuator pairs.

When decentralised velocity feedback loops are implemented in such a way as to generate active damping, both the frequency average vibration and sound radiation of the structure are reduced[8,9], provided an optimal gain is implemented such that the damping action is maximised without pinning the structure at the control positions[13]. The optimally tuned active dampers reduce the amplitudes of the well separated low frequency resonances of the structure and thus the frequency averaged vibration and sound radiation at low frequencies.

In principle, SISO feedback control systems using distributed sensor–actuator pairs specifically designed to minimise the most efficient radiations modes of the radiating structure[14] form the simplest and most convenient solution for active structural acoustic control. However, they normally require

strain transducers, such as piezoelectric transducers, which can not be easily used in matched pairs as sensors and actuators because feed-through effects that limit the stability of the control loop[15].

In conclusion, decentralised MIMO systems offer a good compromise between the fully coupled MIMO and the distributed transducers SISO control systems. The main issue of this strategy is the design of collocated and dual sensor actuator pairs. The purpose of this paper is to discuss the design of one feedback active control unit to be used in a decentralised MIMO control system arranged on a thin panel in order to control both its vibration and sound radiation. The feedback control unit consists of an inertial force actuator with a velocity sensor at its base. The study is focussed on the stability and control performance properties of four feedback control functions which, using the velocity error signal implements[5]:

1. Proportional Control for implementation of Velocity Feedback;
2. Integral Control for implementation of Displacement Feedback;
3. Derivative Control for implementation of Acceleration Feedback and
4. PID Control (Proportional–Integral–Derivative Feedback Control).

The following section presents the model problem considered in this paper. Then, in Sections 3 and 4 the stability and control performance properties of the four control functions are assessed.

2 MODEL PROBLEM

As schematically shown in Figure 1, the study presented in this paper considers a simply supported plate with one feedback control unit which consists of an inertial actuator with an ideal velocity sensor at its base. The inertial actuator is made of a magnet-coil linear motor that reacts off a proof mass mounted on a spring. As a result a point force actuation is generated at the base of the actuator. Normally the coil is fixed to the base of the actuator and the magnet is used as the proof mass. The plate is assumed to be excited by a primary force f_p.

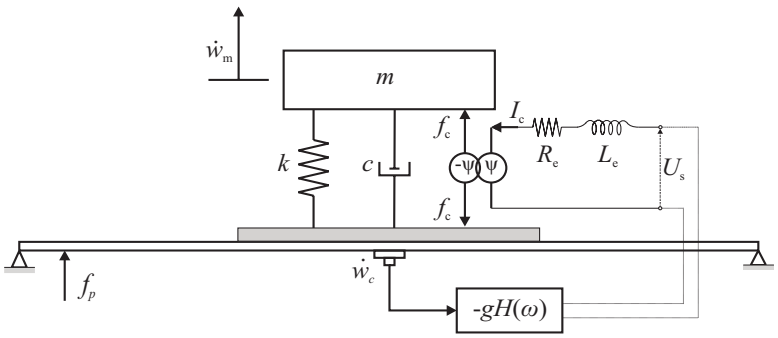

Figure 1. Scheme of an inertial electro–dynamic actuator and velocity sensor control unit mounted on a simple supported plate

The coil–magnet electrodynamic actuator is modelled in terms of a resistance R_e and inductance L_e for the coil. The actuation reactive force f_c and back e.m.f. in the coil are given by the voice coil coefficient ψ[5]. Two control arrangements are considered where the actuator is either current driven or voltage driven. According to Biot–Savart's law, the reactive force f_c generated by the coil–magnet system is directly proportional to the driving current for the current control case. In contrast, for the voltage control, the reactive force f_c is proportional to the resultant voltage in the driving coil because of the back e.m.f. effect generated by the relative motion between the magnet and the coil. The details of the fully coupled model based on mechanical and electrical mobility/impedance functions are given in reference[16].

The force f_a transmitted to the base of the actuator is given by the product of the proof mass and its acceleration. Thus, as shown by the two plots in Figure 2, the spectrum of the transmitted force increases monotonically with frequency up to a maximum value at the resonance frequency of the

mass-spring actuator system, which in the case under study is aproximately 10 Hz. At higher frequencies, the transmitted force f_a levels down to a value that is approximately constant and equal to the reactive force f_c generated by the coil–magnet system[16].

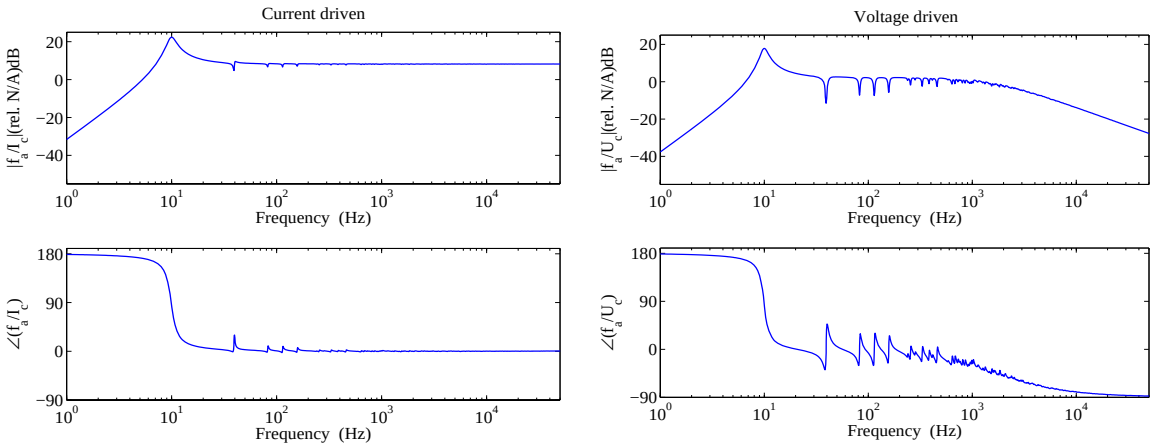

Figure 2: Force transmitted to the base structure per unit driving current (left) and voltage (right)

A number of troughs are shown in correspondence to the low frequency resonances of the plate, which are due to the fact that at these resonance frequencies the plate produces little reaction to the actuator excitation. This effect is more pronounced for the voltage driven actuator. At frequencies below the fundamental resonance frequency of the actuator, the transmitted force is out of the phase with the control signal while, at frequencies above the actuator resonance, it is in phase with the control signal. Above about 1 kHz, the transmitted force by the voltage driven actuator is characterised by an amplitude roll off and a constant phase lag which are due to the inductance of the driving coil. This tends to decrease the current in the driving coil, consequently lowering the actuation force.

3 STABILITY ANALYSIS

A critical problem for the implementation of feedback control systems is stability. To address this problem, several graphical techniques have been developed for Single Input Single Output control schemes. In this paper the Bode and Nyquist plots of the open loop sensor actuator response function are used with reference to the Nyquist stability criterion[5,16,17].

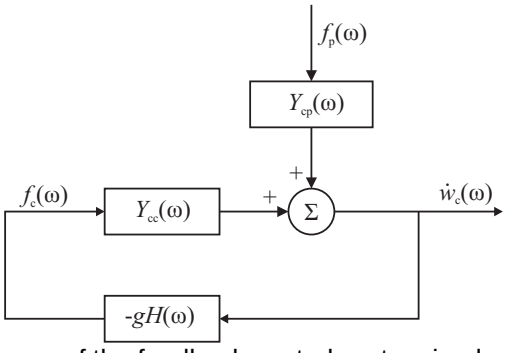

Figure 3. Block diagram of the feedback control system implemented on the plate

The response of the feedback control loop can be formulated in terms of a classic disturbance rejection control scheme as shown in Figure 1. Thus the response at the control position is given by:

$$\dot{w}_c = \frac{Y_{cp}}{1 + gH(\omega)Y_{cc}} f_p \qquad (1)$$

where Y_{cp} is the transfer function between the error sensor and the primary force, $H(\omega)$ is the control function and $G_{cc}=H(\omega)Y_{cc}$ is the open loop frequency response function (FRF) between the error sensor and either the current or voltage control input. These response functions have been derived from the fully coupled model of the plate and electro–dynamic inertial actuator[16]. According to equation 1, if Re{G_{cc}}>0, then $\dot{w}_c / f_p < 1$ for any control gain and frequency. Thus, assuming the control function is a fixed gain, in order to have an unconditionally stable control system, the open loop sensor–actuator FRF G_{cc} must be real positive definite. In this case, the Nyquist plot of G_{cc} occupies the right hand side quadrants as ω varies from –∞ to +∞ and thus the Nyquist instability point (-1+j0) is never encircled regardless of the control gain[5,7,17]. Also, the Bode plot of G_{cc} is minimum phase in the range between ±90°. In order to have a real positive open loop FRF G_{cc}, the sensor–actuator transducers must be collocated and dual[10,11].

3.1 Proportional Control–Velocity feedback

In order to implement negative velocity feedback[12], the output signal from the velocity sensor is fed back to the actuator via a negative proportional control function; $H(\omega) = -g$

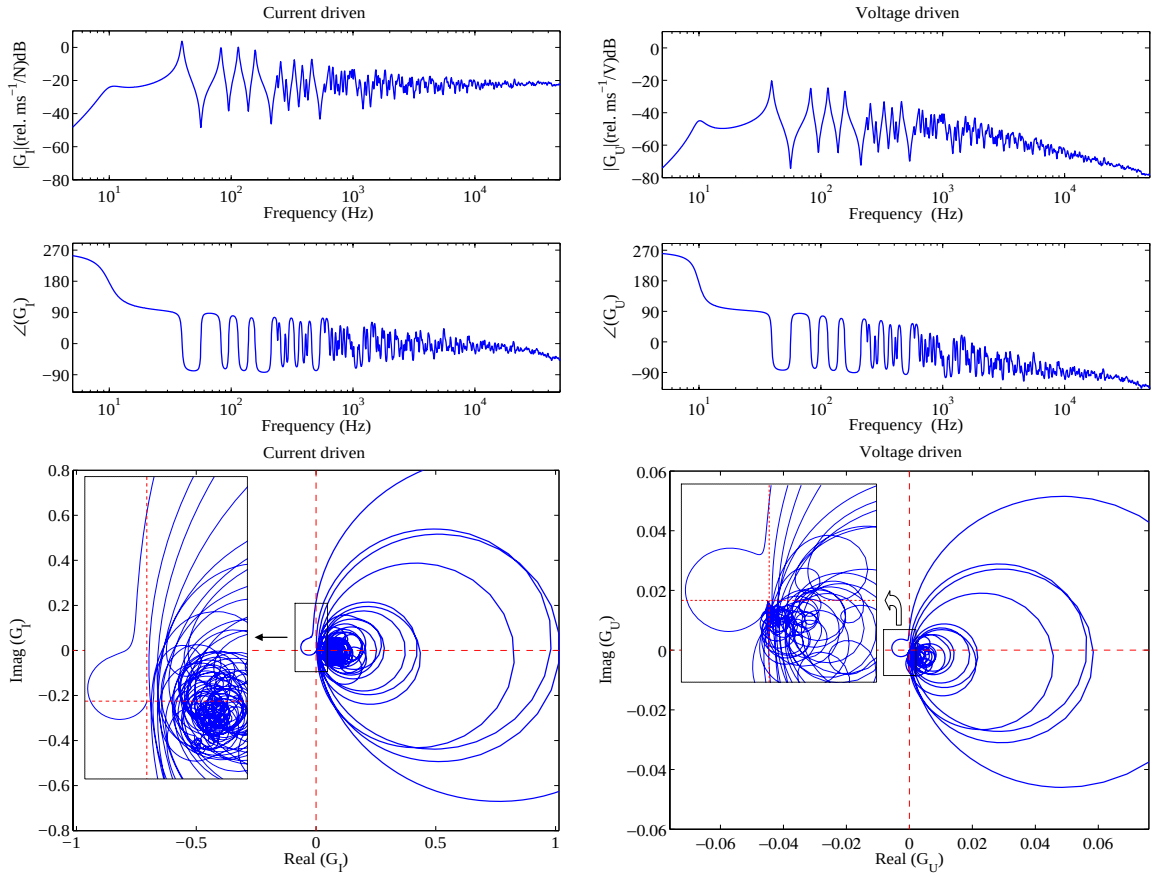

Figure 4. Bode (top plots) and Nyquist plots (bottom plots) of the open loop sensor–actuator FRF when a Proportional feedback loop is used for current (left plots) and voltage (right plots) control

The Bode plots in Figure 4 indicate that, for both current and voltage driven actuators, the phase of the open loop sensor–actuator FRF starts from +270° at low frequency, drops to +90° beyond the resonance of the actuator and then oscillates between +90° and –90° for the resonances of the plate. The first 180° phase drop, from 270° to 90°, is due to the inertial electro–dynamic actuator which, as shown in Figure 2, transmits a force f_a to the plate which is 180° out of phase with the actuator driving signal below the actuator resonance frequency. In the voltage control case, at higher frequencies

above 1 KHz, the phase plot goes to values beyond –90° because of the coil inductance. This inductance also decreases the amplitude of the open loop response function.

The loci of the open loop sensor–actuator FRF shown in Figure 4 is characterised by one circle in the left hand side quadrants which is due to the resonance of the actuator, and many circles in the right hand side quadrants which are due to the resonances of the plate. Thus the control system is bound to be only conditionally stable since, for relatively high control gains, the circle on the left hand side due to the fundamental resonance of the actuator can enclose the Nyquist instability point.

In conclusion in order to get a stable proportional velocity control loop with large control gains it is necessary to have a low-amplitude actuator resonance frequency. This condition is also important to minimise the control spillover effects at low frequencies around the resonance of the actuator. This low-amplitude resonance of the actuator is normally obtained by designing an actuator with natural frequency well below the first resonance of the structure. There is however an intrinsic limit to achieve this result since the stiffness of the actuator must be high enough to hold the mass without a big static deflection; therefore a compromise must be found between a stiff enough spring to support the static weigh of the suspended mass and a soft enough spring to guarantee a low fundamental resonance frequency of the actuator[18]. Further improvements can be obtained by adding and internal velocity feedback loop to the actuator which generates relative active damping in the actuator that reduces the amplitude of its resonance[19]. Alternatively a very soft mount can be used in combination with an integral displacement feedback control loop, which acts as a self levelling system that limits the extent of the static displacement[20].

3.2 Integral Control–Displacement feedback

In order to implement negative displacement feedback, the output signal from the velocity sensor is fed back to the actuator via a negative integral control function; $H(\omega) = -g / j\omega$

The Bode plots in Figure 5 indicate that the phase of the open loop sensor–actuator FRF starts from +180°, drops to 0° at the resonance of the inertial actuator and then oscillates between 0 and –180° at higher frequencies above the first resonance of the plate. As discussed above, this is due to the actuator dynamics which, as shown in Figure 2, transmit to the plate a force f_a which is 180° out of phase with the driving signal at frequencies below its fundamental resonance. In this control case, the amplitude of the open loop tends to decrease with frequency because of the integration $1/j\omega$. For the voltage–driven inertial actuator this effect is even higher because of the coil inductance which introduces an extra phase lag and amplitude drop at higher frequencies.

The loci of the open loop sensor–actuator RFR shown in Figure 5 is characterised by one circle in the top side quadrants, which is due to the actuator–resonance, and many other circles on the bottom side quadrants which are due to the resonance of the plate. Thus, compared to proportional control, the effect of integral control is to rotate in the clockwise direction the locus in the Nyquist plot and to reduce the size of the higher frequencies circles. This should improve the stability of the system since the circle due to the actuator resonance no longer lies exactly along the real negative axis. However, as shown by the magnified plot, for very low frequencies, this circle gets very close to the negative real axis. Although it never crosses the negative real axis, it may cause instabilities when small external perturbations slightly change the dynamics of the actuator. The circles due to the plate resonances are moved to the bottom half of the Nyquist plots so that they pass close to the Nyquist critical point at higher frequencies. In principle, when the actuator is current driven, the locus of the open loop sensor–actuator FRF does not cross the negative real axis and thus guarantees an unconditionally stable system. However when the actuator is voltage driven, because of the extra phase shift introduced by the inductance effect of the driving coil; as shown by the magnified plot, it crosses the negative real axis so that stable control is guaranteed only for a limited range of feedback control gains.

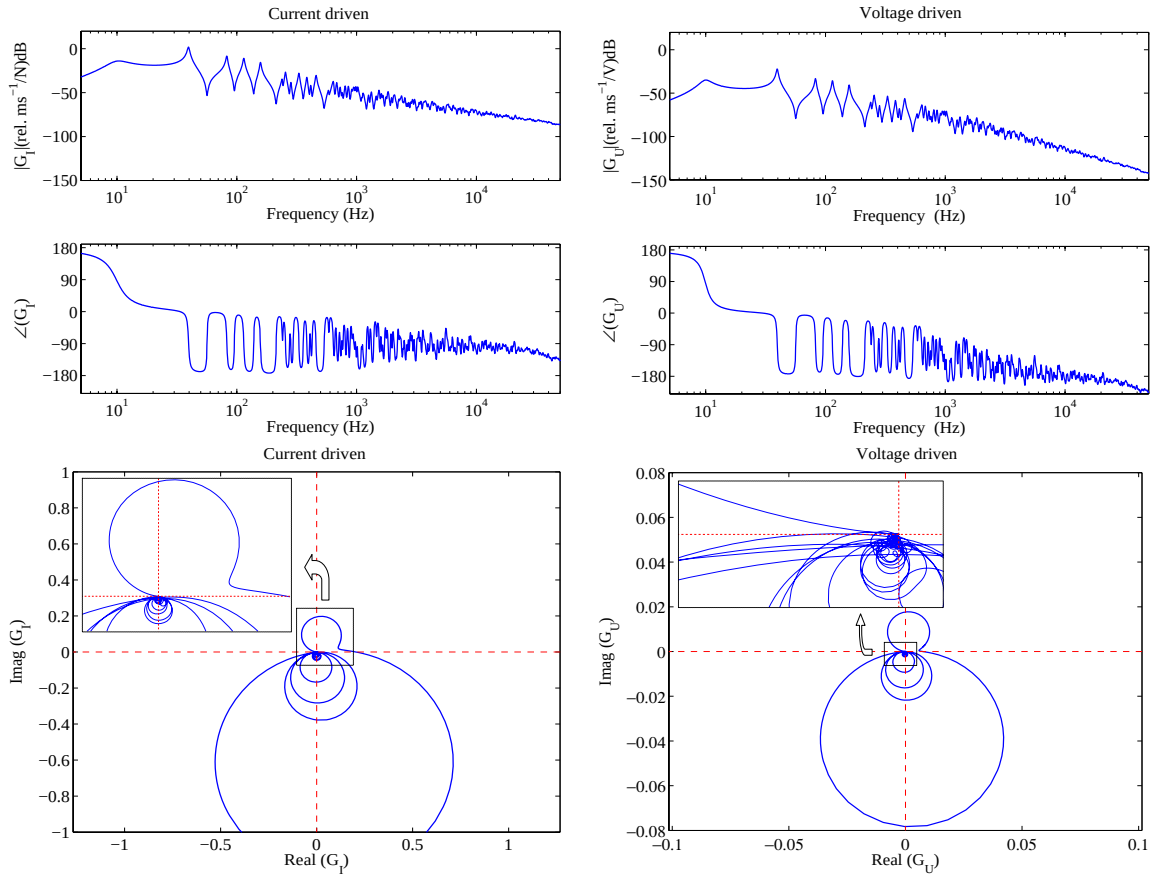

Figure 5. Frequency response functions; Bode plots (tops plots) and Nyquist plots (bottoms plots) of the open loop sensor–actuator FRF when a Integral Control is used for current (left plots) and voltage (right plots) driven

In general, the vicinity, of both top and bottom circles to the negative real axis makes integral feedback quite difficult to implement. Even small phase lead or lag effects due to external disturbances will cause the top and bottom circles to cross the negative real axis and thus only a limited range of control gains can be implemented in a stable control loop. Also, control spillover effects are likely to occur at those frequencies such that the Nyquist plot enters the circle of radius one centered at the critical point (-1+j0)[5,6,17].

3.3 Derivative Control–Acceleration feedback

In order to implement negative acceleration feedback, the output signal from the velocity sensor is fed back to the actuator via a negative derivative control function; $H(\omega) = -j\,\omega\,g$

In this case, the Bode plots in Figure 6 indicate that the phase of the open loop sensor–actuator FRF starts from +360° and drops to +180° at the resonance of the inertial actuator. This is because, as shown in Figure 2, the transmitted force f_a flips sign with the control signal. At higher frequencies, above the first resonance of the plate, the phase oscillates between 180° and 0°. The implementation of a derivative control function produces a constant rise of the open loop sensor–actuator FRF with frequency. This effect is however mitigated by the coil inductance effect of the voltage driven system.

The loci of the loop sensor–actuator FRF shown in Figure 6 are characterised by one circle on the bottom quadrants, which is due to the resonance of the actuator, and other circles for the resonances of the plate on the top quadrants. Thus, in contrast to proportional control, the effect of derivative control is to rotate the Nyquist plot in the anti-clockwise direction and to enlarge the higher frequencies circles. In principle this should also improve the stability of the system since the circle

due to the actuator resonance no longer lies exactly along the real negative axis. However, in this case, as shown by the magnified plot, the transition from the circle due to the actuator resonance and the circle of the first resonance of the plate crosses the negative real axis, so that the control loop is bound to be stable only for a limited range of feedback control gains. Also, control spillover is likely to occur at low frequencies since the locus enters the circle of radius one and centre (-1+j0). For current driven actuators, the higher frequency part of the locus tends to form a sequence of circles along the imaginary axis so that the complex part rises monotonically. This effect is less pronounced when the actuator is voltage driven because of the coil inductance which tends to decrease the amplitude and to enhance the phase lag of the open loop FRF. In any case having a control system with such a large locus of the open-loop sensor-actuator FRF in the higher frequency range could be a problem since high frequency phase lags introduced by the control circuit may lead to instabilities even for very small control gains.

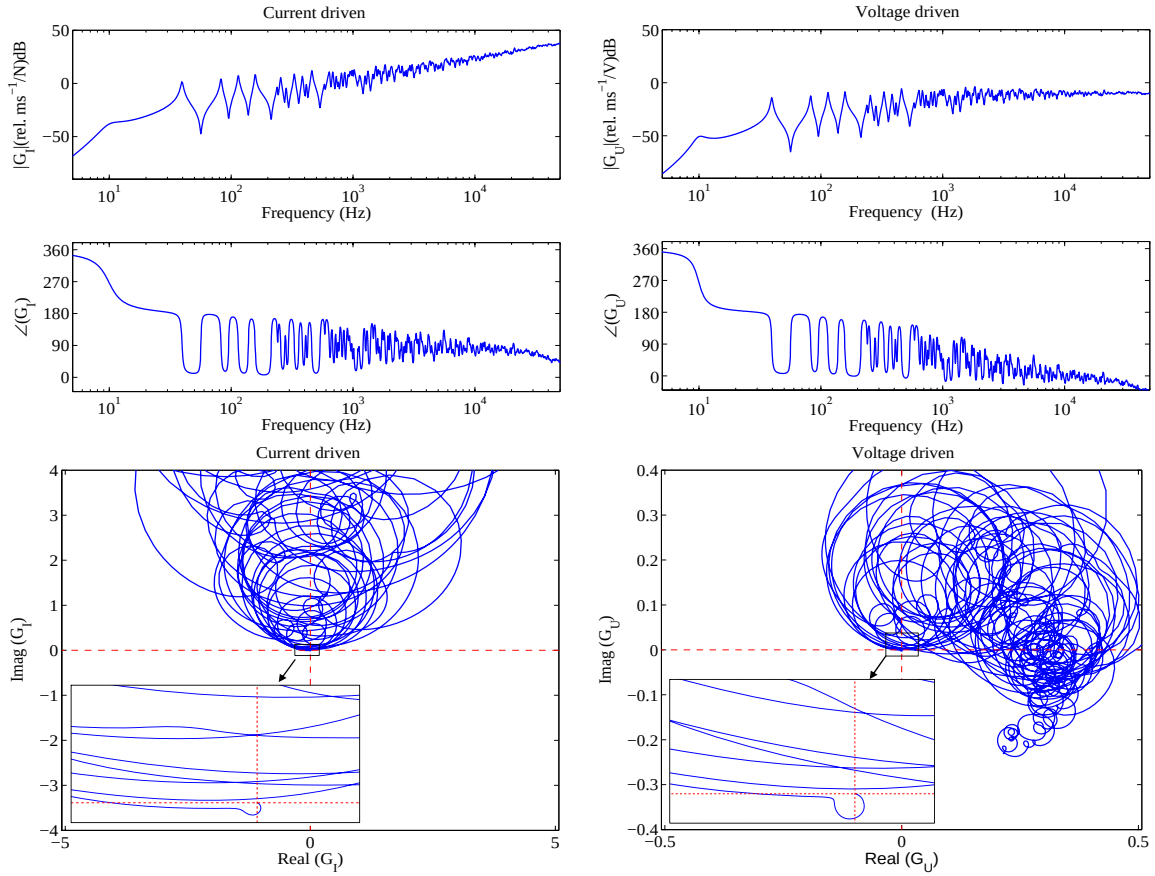

Figure 6. Frequency response functions; Bode plots (tops plots) and Nyquist plots (bottoms plots) of the open loop sensor–actuator FRF when a Derivative Control is used for current (left plots) and voltage (right plots) driven

3.4 PID Control

The effects generated by a combination of negative displacement, negative velocity and negative acceleration feedback are also studied in this paper. In this case the output signal from the velocity control sensor is fed back to the control force actuator via a negative combination of Proportional–Integral–Derivative functions: $H(\omega) = -g\{k_P + k_I/j\omega + j\omega k_D\}$. The integral and derivative control parameters, k_I and k_D have been tuned with reference to the first resonance of the plate in such a way as that below this resonance the control is set to be integral controlled, at resonance to be proportional controlled and above resonance to be derivative controlled. Also k_D has been set to 1.

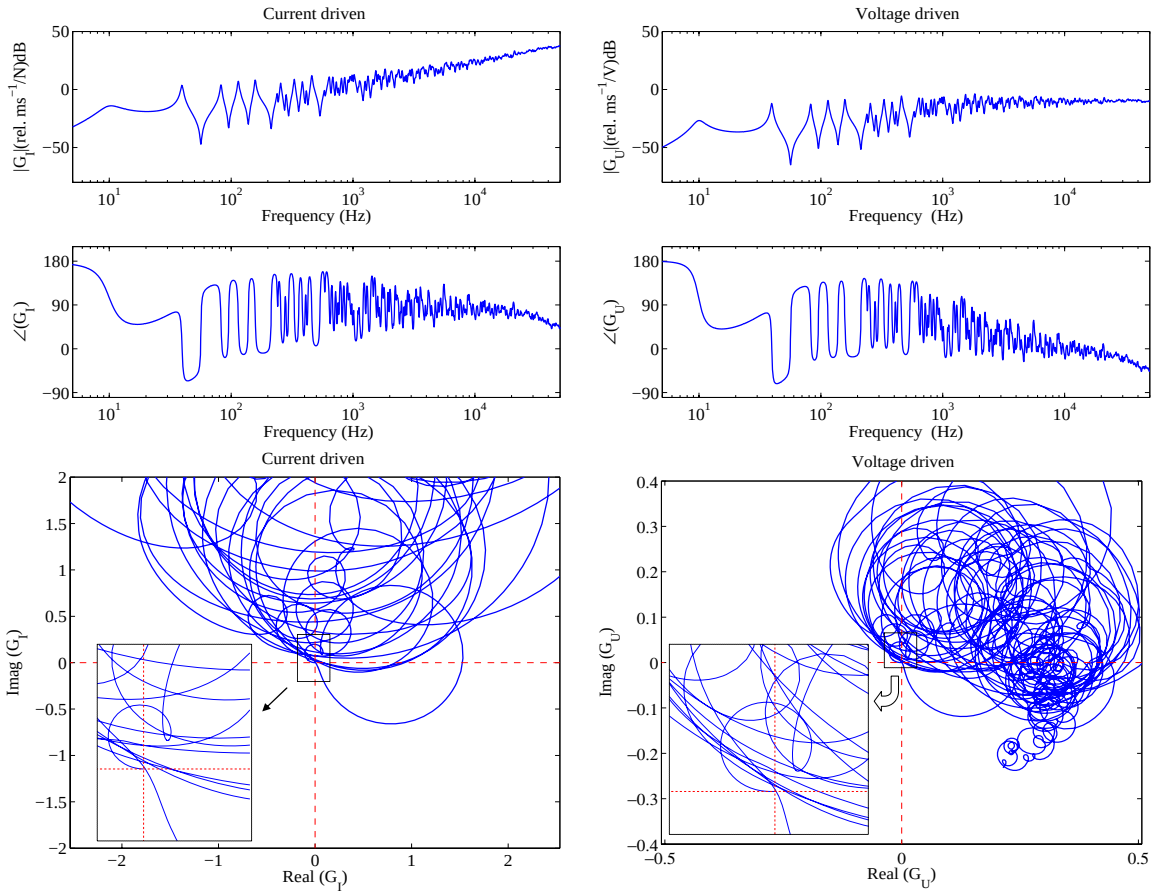

Figure 7. Frequency response functions; Bode plots (tops plots) and Nyquist plots (bottoms plots) of the open loop sensor–actuator FRF when a PID Control is used for current (left plots) and voltage (right plots) driven

In this case, the Bode plots in Figure 7 indicate that the phase of the open loop sensor–actuator FRF starts from +180°, drops almost to 0°, oscillates between –90° and +90° once and then oscillates between 0° and 180° above the first resonance of the plate. Thus, the integral control component tends to produce a +90° phase lead effect at lower frequencies and the derivative control component produces a -90° phase lag at higher frequencies above the first resonance of the plate. As found in the previous case, the derivative effect produce a constant increase of the amplitude of the open loop FRF with frequency, which is less pronounce with the voltage driven actuator because of the driving coil inductance effect.

The loci of the loop sensor–actuator FRFs in Figure 7 indicates that, at low frequency below the first resonance of the plate, the integral control effect in the PID controller locates the locus–circle for the actuator resonance in the top quadrants as seen in Figure 5 for the purely integral control case (see magnified plot). Also, the proportional effect in the PID controller locates the locus–circle for the first resonance of the plate on the right hand side quadrants as typically happens with purely proportional control (see Figure 4). At higher frequencies, the derivative effect in the PID controller moves the circles to the top quadrants and produces the typical amplification effect proportional to frequency of purely derivative control. When the voltage–driven inertial actuator is used, then it is found that the typical higher frequencies phase lag and amplitude drop effects which is counterbalanced by the amplification effect of the derivative control. In summary this PID control function is bound to be unconditionally stable. At very low frequencies the locus-circle related to the actuator resonance can pass close to the Nyquist critical point when large control gains are implemented. This has two drawbacks since control spillover is likely to occur and also instability effects may be generated even by small disturbances at low frequencies.

4 CONTROL PERFORMANCES

When distributed flexible systems are considered, the overall vibration of the plate can be assessed in terms of its time-averaged total kinetic energy which is given by[16]:

$$K = \frac{1}{4} M \left| f_p \right|^2 \mathbf{a}^H \mathbf{a} \qquad (2)$$

where M is the mass of the plate and **a** is a column vector with the modal amplitudes of the plate generated by the action of both primary excitation and control actuator when the feedback control loop is closed. The complete formulation to derive equation 2 can be found in reference[16].

Figure 8 shows the kinetic energy in the frequency range between 0 and 1 kHz for the two control arrangements and the four control functions. When there is no control, the spectrum of the kinetic energy is characterised by well separated resonances which are determined by the modes of the plate. It is interesting to note that there is nearly no peak for the actuator resonance at 10 Hz.

Considering first the effect of proportional control, for both cases of current and voltage driven control, it is found that when the control gain raises the response at the first few resonance frequencies of the panel are decreased. This is due to the active damping effect of the control system which tends to reduce the resonant response of the lower order modes which are well coupled with the control actuator. As expected, the resonance due to the actuator produces a control spillover effect so that, although the control system is stable, the peak of the actuator resonance is amplified rather than lowered[18]. When very large control gains are implemented, the spectrum of the kinetic energy turns back to that in the case of no control except that the first few resonances of the panel are brought up in frequency[8,9]. This is a well known phenomenon which is due to the fact that for very large feedback control gains the vibration of the plate is pinned at the control position and thus no more active damping is introduced in the plate itself. Thus, for very high control gains the response becomes that of a lightly damped plate with a constraint at the control position[13]. Comparing the effects produced by the current and voltage driven control loops, the two plots in Figure 8 indicate that the control spillover effect at the fundamental resonance of the actuator is more pronounced for the voltage control system. This is probably due to the high frequency filtering effect on the open loop sensor-actuator FRF (see Figure 4) so that in order to generate the same active damping levels as with the current driven control system, much larger control gains must be implemented and thus much larger control spillover effects are generated at the fundamental resonance frequency.

In summary, considering the thick solid lines of the two plots in Figure 9, the frequency averaged total kinetic energy monotonically decreases as the control gains raises from zero up to the optimal control gain where the maximum reduction of about 2 dB is obtained (note that this reduction is greater when several decentralised control units are used together). For higher gains, the curve have been interrupted because the system would go unstable values.

The second row of plots in Figure 8 shows that the integral control, which implements active stiffness, tends to move up the resonances of the panel. The control spillover effect is relatively smaller than that found with the proportional control system and occurs at much lower frequency than that when the feedback control loop is left open. Nevertheless comparing these results with those obtained with the proportional control system, it is evident that with integral control there is a consistent reduction of vibration only at frequencies below the first resonance of the panel where the response of the panel is indeed controlled by stiffness. At higher frequencies there is a shift of the resonance frequencies of the panel low order modes which may result into vibration reductions or enhancements in narrow frequency bands. This trend is confirmed by the plots in Figures 9 (dashed lines) which highlights how the integral control produces smaller maximum reductions of the frequency averaged kinetic energy of the panel although this maximum is obtained with smaller control gains. The dashed line in the plot for the voltage driven actuator in Figure 9 is interrupted because the closed loop would be unstable for higher control gains.

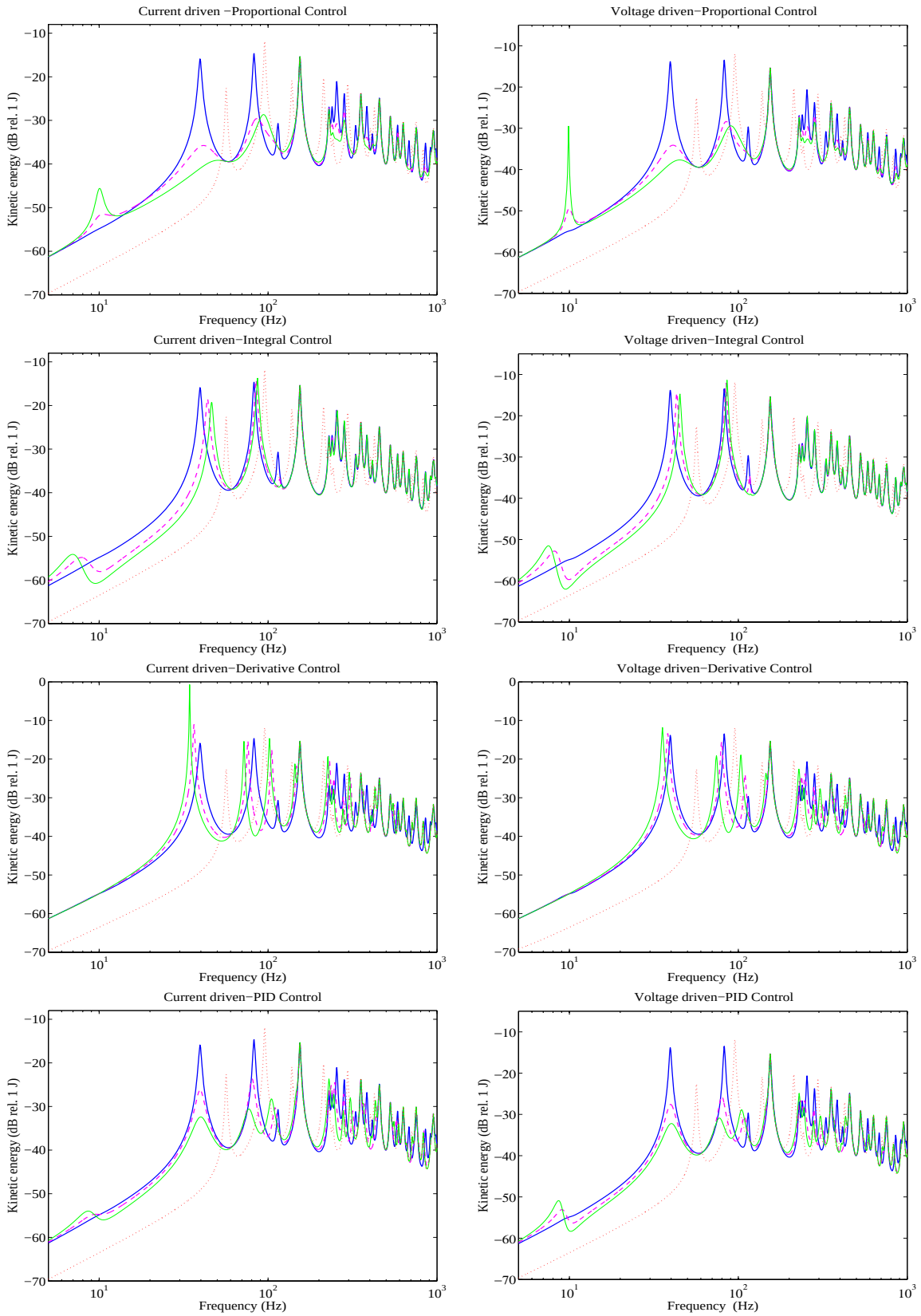

Figure 8. Total flexural kinetic energy of the plate when the control actuator is current and voltage driven (respectively left- and right-hand side plots) and Proportional, Integral, Derivative and PID control functions are implemented with a set or rising control gains

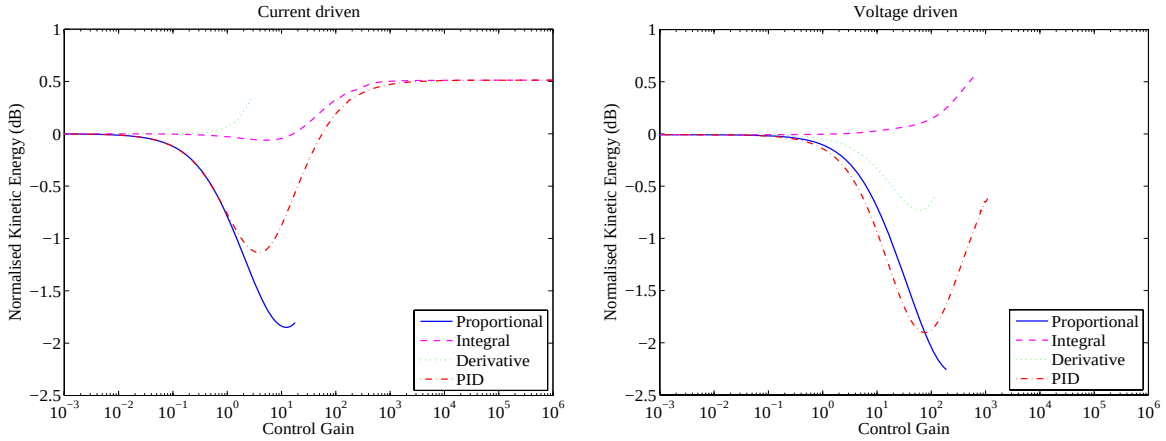

Figure 9. Normalised Frequency Averaged Total Kinetic Energy in the range 0 – 1 kHz as a function of the control gain in the current and voltage driven control system

The third row of plots in Figure 8 shows the effect of derivative control that implement active mass. The overall result is a shift of the resonance frequencies of the panel which in this case are decreased. The dotted lines in Figure 9 show that in this case the reduction of the frequency averaged total kinetic energy is negligible for the current driven control system and very small for the voltage driven control system. This is due to the fact that the mass control system acts in a frequency range where the response of the panel is characterised by resonance responses which are determined by stiffness and mass controlled response respectively below and above the resonance frequency. Thus the active mass effect does not produce an effective reduction of the vibration in a wide frequency band. The dotted lines in Figure 9 are interrupted for relatively low control gains since, as highlighted in the previous section the control loop goes unstable for relatively small control gains.

The bottom row in Figure 8 shows the effect of PID control. The integral component in the controller reduces the vibration of the panel at frequencies below the first resonance. The proportional component is then effective at the first and second resonances of the plate. As found in the previous case the proportional component produces some control effects only in narrow band frequencies. Thus, the reduction of the total kinetic energy averaged in a range between 0 and 1 kHz is lower to that obtained with proportional control (dashed-dotted line). However, the reduction in the frequency range between 0 and 100 Hz is much higher. This type of control unit is specifically tuned to produce active damping on a relatively small frequency band. Thus, it may be possible that, by using an array of these control systems centred at different frequencies, a relatively higher control performance is generated than by using an array with proportional feedback control loops.

5 CONCLUSION

This paper has presented a simulation study about the stability and control performance of a feedback control unit that is used to implement decentralised MIMO control in smart panels. The control unit consist of an inertial actuator with a velocity sensor at its base. Four control functions have been considered: a) Proportional, b) Integral c) Derivative and d) PID.

The stability analysis has highlighted that when proportional control is implemented then the locus of the sensor–actuator open loop response function is characterised by one circle in the left hand side quadrants of the Nyquist plot, which is due to the actuator resonance, and many other circles in the right hand side quadrants which are due to the plate resonances. Thus the system is bound to be conditionally stable with gain margin dependent on the amplitude of the actuator resonance. Integral and Derivative control functions produce a rotation of 90^{o}, respectively in the clockwise and in the anti-clockwise directions of the locus. In principle this should reduce the stability problem but the integration and derivative effects on the amplitude of the open loop response function produce some limitations on the maximum control gains that guarantee stability.

The control performance analysis has shown that, when the error sensor measures velocity, proportional control implements active damping so that the response of the panel is reduced at the resonance frequencies. Integral and derivative control produces active stiffness and active mass respectively so that the resonance frequencies of the plate are moved up and down respectively and vibration reductions are obtained in the frequency bands where the response of the plate is stiffness and mass controlled respectively. The PID control scheme provides a combination of active stiffness, damping and mass effects which produces good control results in small frequency bands on which the PID function is tuned.

6 ACKNOWLEDGEMENTS

The work done by C. González Díaz for this project was supported by the “Early Stage Training site Marie Curie” programme for the “European Doctorate in Sound and Vibration Studies” (EDSVS), which is funded by the European Commission.

7 REFERENCES

1. F.J.Fahy. Sound and Structural Vibration. 1985. London, Academic Press.
2. C.R.Fuller, S. J. Elliott and P. A. Nelson. Active Control of Vibration. 1996. New York, Academic P.
3. P.A.Nelson and S.J.Elliott. Active Control of Sound. 1992. New York, Academic Press.
4. S.J.Elliott. Signal Processing for Active Control. 1. 2001. London, Academic Press.
5. A.Preumont. Vibration control of active structures. 2. 2002. London, Kluwer Academic.
6. R.L.Clark, W. R. Saunders and G. P. Gibbs. Adaptive Structures. 1st Edition. 1998. New York, John Wiley & Sons, Inc.
7. B.Petitjean and I.Legrain. Feedback controllers for active vibration suppression. Journal of Structural Control **3**[1-2], 111-127. 1996.
8. P.Gardonio, E. Bianchi and S. J. Elliott. Smart panel with multiple decentralised units for the control of sound transmission. Part I: theoretical predictions. Part II: design of the decentralised control units. Part III: control system implementation. Journal of Sound and Vibration No. 274 pp 163-232, 2004.
9. Elliott, S. J., Gardonio, P., Sors, Thomas C., and Brennan, M. J. Active vibroacoustic control with multiple local feedback loops. The Journal of the Acoustical Society of America 111[2], 908-915. 2002.
10. J.Q.Sun. Some observations on physical duality and collocation of structural control sensors and actuators. Journal of Sound and Vibration 194, 765-770. 1996.
11. Jayachandran, V., Sun, J. Q. Unconditional stability domains of structural control systems using dual actuator-sensor pairs. Journal of Sound and Vibration 208[1], 159-166. 1997. Academic P.
12. M.J.Balas. Direct velocity control of large space structures. Journal of Guidance and Control 2, 252-253. 1979.
13. Gardonio, P and Elliott, J. Modal response of a beam with a sensor-actuator pair for the implementation of velocity feedback control. Journal of Sound and Vibration 284[1-2], 1-22. 7-6-2005.
14. Johnson, M. E. and Elliott, S. J. Active control of sound radiation using volume velocity cancellation. Journal of the Acoustical Society of America 98[4], 2174-2186. 1995.
15. Gardonio, P., Lee, Y. S., Elliott, S. J., and Debost, S. Analysis and measurement of a matched volume velocity sensor and uniform force actuator for active structural acoustic control. JASA 110[6], 3025-3031. 2001.
16. C.González Díaz and P.Gardonio. Proportional, Integral, Derivative, PID-, PI-, and PD- Velocity Feedback Control with Inertial Actuators. 2005. ISVR Technical Memorandum No.956.
17. L.Meirovitch. Dynamics and Control of Structures. 1990. New York, John Wiley & Sons.
18. Elliott, S. J., Serrand, M., and Gardonio, P. Feedback Stability Limits for Active Isolation Systems with Reactive and Inertial Actuators. Journal of Vibration and Acoustics 123[2], 250-261. 2001. ASME.
19. C.Paulitsh, P. Gardonio and S. J. Elliott. Active vibration control using an inertial actuator with internal damping. Journal of the Acoustical Society of America (in print) . 2006.
20. Benassi, L. and Elliott, S. J. Active vibration isolation using an inertial actuator with local displacement feedback control. Journal of Sound and Vibration 278[4-5], 705-724. 22-12-2004.